




Research Paper

Improving the Resiliency of Electrical Distribution Networks by Optimal Embedding Switchable Capacitor Banks in Microgrids Based on a Convex Model

Hesam addin Yousefian , Abolfazl Jalilvand , and Amir Bagheri* 

Department of Electrical Engineering, University of Zanjan, Zanjan, Iran.

Abstract— The importance of durability and sustainability in electrical energy, particularly in emergency conditions, has led to the development of operational techniques aimed at improving the serviceability of electrical distribution networks (EDNs). Operating the electrical distribution network as a smaller, islanded system in the form of a microgrid (MG) is one of the key enhancement methods that has gained attention. Each microgrid is subject to specific constraints that must be addressed. Moreover, the increasing penetration of renewable distributed generation (DG) units introduces additional limitations. The limited reactive power generation by synchronous DGs within each MG leads to higher levels of load shedding. This paper investigates the resiliency of EDNs with a focus on microgrid formation strategies. To achieve this, the limitations of MG formation, including the use of wind turbines, photovoltaic units as renewable DGs, and energy storage systems, are considered. The application of switchable capacitor banks (SCBs) is proposed and formulated to meet these requirements. All equations are convex and formulated within the GAMS environment using mixed-integer quadratically-constrained programming (MIQCP). The proposed framework is evaluated using the IEEE 69-node test system, considering various case studies. The results show that the economic deployment of SCBs in the MG formation of the studied EDN leads to a reduction of the objective function by approximately 13.6%, a loss reduction of about 26.1%, and a significant increase in the penetration of renewable resources by 285.6%.

Keywords—Resiliency, microgrid, electrical distribution network, switchable capacitor banks, renewable DGs, convex model.

NOMENCLATURE

Abbreviations

EDN	Electrical distribution network
ESS	Energy storage system
HILP	High impact low probability
MG	Microgrid
MIQCP	Mixed-integer quadratically-constrained programming
OF	Objective function
SCB	Switchable capacitor bank
SDG	Synchronous distributed generation

Indices

i, j	Buses
l	Connecting line of two adjacent buses i and j
m	Micro-grids
t	Time

Parameters

A_{li}	The $li - th$ element of the bus-line matrix. It is equal to 1 if bus i is the sending bus of line l and -1 if bus i is receiving one. Otherwise, it will be zero.
----------	--

B_{li}	The li -th element of the bus-line matrix. It is equal to 0 if bus i is the sending bus of line l and 1 otherwise.
$bigM$	A big number
f_i	Load priority factor
FF	Filling factor of PV units
$flow_{min}/flow_{max}$	Minimum/maximum hypothetical active power that can be passed through lines
I_i^g	Output current of PV units
$I_{i,j}^{max}$	Peak thermal capacity of lines
I_{MPP}	The highest level power point tracking current in PV units
I_{sh}^{pv}	Short-circuit current of PV units
K_i	Current temperature coefficient of PV units
K_v	Voltage temperature coefficient of PV units
N_s	The steps number of SCBs
N_{max}^{CAP}	Capacity of switchable capacitor banks (SCBs)
N_{max}^{Cap}	The most available number of (SCBs) in the system
N_{max}^{DG}	Capacity of synchronous DGs
N_{max}^{DG}	The most available number of synchronous DGs in the system
N_{max}^{ESS}	The most available number of ESSs in the system
N_{max}^{PV}	The most available number of PV unites in the system
N_{max}^W	The most available number of wind turbines in the system
N_{OT}	Rated operating temperature in PV units
N_{pv}	Number of PV cells
P_i^L/Q_i^L	Maximum demand of active/reactive load
$P_{i,t}^{pv,Capacity}$	Maximum power capacity of PV units
$P_{i,t}^{w,Capacity}$	Maximum active power capacity of wind turbines
P_{max}^{ESS}	Maximum active power of ESSs
$P_{min}^{net}/P_{max}^{net}$	Minimum/maximum active power passing through

Received: 06 Jul. 2024

Revised: 31 Aug. 2024

Accepted: 08 Sept. 2024

*Corresponding author:

E-mail: a.bagheri@znu.ac.ir (A. Bagheri)

DOI: 10.22098/joape.2024.15405.2180

This work is licensed under a [Creative Commons Attribution-NonCommercial 4.0 International License](https://creativecommons.org/licenses/by-nc/4.0/).

Copyright © 2025 University of Mohaghegh Ardabili.

	lines
P_{rated}^w	Rated power of wind turbines
PF_{DG}	Power factor of synchronous DGs
$Q_{min}^{net}/Q_{max}^{net}$	Minimum/maximum reactive power passing through lines
R_l^{Line}	Resistance of line l
S_{it}	Solar radiation intensity
SOC_{max}	Maximum state of charge of ESSs
T_t^A	Ambient temperature
T_t^{cg}	Temperature of PV units
V_t^g	Output voltage of PV units
V_t^{wind}	Instantaneous wind speed at time t
V_{c-in}/V_{c-out}	Cut-in/cut-out speeds of wind turbines
V_{min}/V_{max}	Minimum/maximum voltage of buses
V_{MPP}	The highest level of power point tracking voltage in PV units
V_{oc}^{pv}	Open-circuit voltage of PV units
V_{rated}	Nominal speed of wind turbine
$VOLL$	Value of loss of loads
X_l^{Line}	Reactance of line l
η_{ch}/η_{dch}	Efficiency of ESSs either in charging or discharging modes
σ_t	Coefficient of load in a day
Series	
Ω_L	Series of branches
Ω_N	Series of buses
Ω_T	Series of time
Ω_{MG}	Series of micro-grids
Ω_{PQ}	Series of PQ buses
Variables	
$a_{i,m}$	Binary variable denoting the existence of bus i in micro-grid m
$C_{i,j,t}$	Square of current of line i, j at time t
CAP_i	Binary variable denoting whether an SCBs is placed at bus i (1) or not (0)
$CH_{i,t}$	Binary variable denoting whether charging of a placed energy storage unit at bus i (1) or not (0) at time t
$DCH_{i,t}$	Binary variable denoting whether discharging of a placed energy storage unit at bus i (1) or not (0) at time t
DG_i	Binary variable denoting whether a DG is placed at bus i (1) or not (0)
$DG_{i,m}^{island}$	Binary variable for the existence of at least one synchronous DG in each micro-grid (1) and (0) otherwise
$DG_{i,m}^{MG}$	Binary variable denoting the existence of DG i in micro-grid m (1) and (0) otherwise
ESS_i	Binary variable denoting whether an energy storage unit is placed at bus i (1) or not (0)
$flow_{i,j,m}$	Hypothetical active power passing through lines
$Gen_{i,m}$	Injected hypothetical active power
$I_{i,j,t}$	Passing current through line i, j at time t
$K1_{i,t}$	Binary variable denoting whether the first step of SCBs at bus i is switched(1) or not (0) at time t
$K2_{i,t}$	Binary variable denoting whether the second step of SCBs at bus i is switched (1) or not (0) at time t
$K3_{i,t}$	Binary variable denoting whether the third step of SCBs at bus i is switched (1) or not (0) at time t
$P_{i,j,t}^{Line}/Q_{i,j,t}^{Line}$	Active/reactive power passing through the lines
$P_{i,t}^{lsh}/Q_{i,t}^{lsh}$	Active/reactive load shedding powers
$P_{i,t}^{PV}$	Active power supplied by PVs
$P_{i,t}^{WT}$	Active power supplied by wind turbines
P_{Total}^L	Total load of system
PV_i	Binary variable denoting whether a PV unit is placed at bus i (1) or not (0)
$Q_{i,t}^{CAP}$	Reactive power supplied by SCBs
$r_{i,j,m}^{pos}/r_{i,j,m}^{neg}$	Positive/negative binary variable used for linearization of absolute function
$SOC_{i,t}$	State of charge for ESSs
$U_{i,j,t}$	Square of voltage of bus
$V_{i,t}$	Magnitude of bus voltage

W_i	Binary variable denoting whether a wind turbine is placed at bus i (1) or not (0)
$X_{i,j,m}$	Binary variable denoting whether line (i, j) is an active branch (1) or not (0) at time t
$X_{i,j,m}^{MG}$	Binary variable of connection/disconnection of lines in micro-grid
$P_{i,t}^G/Q_{i,t}^G$	Active/reactive power injected from the upstream network into the system
$P_{i,t}^{DG}/Q_{i,t}^{DG}$	Active/reactive power supplied by synchronous DGs
OF	Main objective function

1. INTRODUCTION

1.1. Background and motivation

Due to the increasing impact of climate change globally, the concept of EDN resilience has emerged, prompting researchers to explore various techniques to optimally address this challenge. EDN resilience is defined as the ability to maintain network operation during emergency conditions caused by natural disasters (high-impact, low-probability events) [1–3]. A review of the related literature shows that several operational methods have been proposed to improve the resilience of EDNs (as classified in Fig. 1). Among these methods, microgrid (MG) formation stands out as an effective approach for enhancing EDN resilience [1–6].

Several aspects of MG formation have been explored and studied previously. However, operational limitations, such as voltage constraints, conductor thermal capacity, and reactive power limitations, affect the effectiveness of MGs. Various techniques—including DG placement, reconfiguration, energy storage system deployment, parking lots, mobile DGs, and the master-slave technique (which controls the frequency of each MG and ensures its variation remains within a predefined range)—have been proposed and studied to improve MG applicability. Nevertheless, there are still numerous aspects that warrant further investigation in the field of resilience enhancement, with a particular focus on improving MG formation.

1.2. Literature review

Resiliency enhancement of EDNs based on dynamic MG formation is studied in Ref. [4] by considering different boundaries. The proposed multi-microgrid formation is formulated as a mixed-integer linear programming (MILP) problem and is verified on the modified IEEE-123 bus system. At last, it is concluded that more resiliency of EDNs can be achieved by flexible boundaries against fixed boundaries. In Ref. [5], a new expansion planning of EDNs is proposed aiming at load shedding decrease. The proposed objective function includes various installation and operation costs of MG formation. By applying this function, independent MGs can be formed and the resiliency of EDNs considering supplying critical loads and minimizing of costs is achievable. Another framework for resiliency improvement is proposed in [6] based on a multi-objective function and MG formation. The proposed model tries to maximize the load restoration and minimize the operation costs. Demand response programs such as shiftable, curtailable and transferable loads are considered which lead to an increase in resiliency index.

In Ref. [7], a resiliency-oriented analysis of EDNs is fulfilled. Uncertainties of renewable generation, natural disasters, and load demand are also considered. The downside risk constraint in modeling the risk can be mentioned as the main approach of this study. An operation framework of EDNs focusing on multi-microgrids is proposed in Ref. [8]. In this study, a linear decision rule based on microgrids is considered to decrease the solution convergence considering renewable uncertainties. The proposed decentralized scheme is faster and its effectiveness is evaluated on the IEEE 69-bus system. In Ref. [9], a question is exposed to discussion and tried to find the best answer. It is asked whether operating EDNs as active distribution networks is better or as



Fig. 1. Classification of resiliency improvement techniques of electrical distribution network.

islanded MGs. An optimization design for an active distribution network capable of transitioning into a microgrid is proposed. The results testify that operating active distribution networks capable of transitioning into a microgrid can reduce operational costs and increase reliability and resiliency of EDNs. A two-stage energy management system that tries to improve the resiliency of EDNs is introduced in [10]. A new convex formulation for the power flow equation is proposed to limit the computational processing time. Analyzing the results reveals that the resiliency of EDNs is improved by taking into consideration the following three preventive functionalities which are: supplying the high priority of critical loads, reducing the generation amounts of DGs that have high probability of failures, and decreasing the serving of loads to ease the impact of failures. In Ref. [11], a novel topology design of microgrid formation is proposed to improve the resiliency of EDNs. In the proposed method, all the available MG topologies are considered and all the stable MGs are classified according to the predefined maximum line vulnerability rank and degree. The results showed that the mentioned criterion is sufficient in determining the best topology of MGs even in emergency conditions. Resiliency improvement is the main goal of Ref. [12] that is reached by battery electric buses utilization along with other generation resources. Due to this, various simulations are done and the numerous advantages of battery electric buses are concluded as powering up methods in MG formation of EDNs. In Ref. [13], MG performance is improved by proposing a method considering various uncertainties of EDNs. By applying the proposed method, the MG performance is maximized and the optimal configurations are identified even in contingencies. The resiliency of EDNs is improved by a method proposed in Ref. [14]. This method is based on network reconfiguration and identifies optimal structures of systems possessing several faults. Another metaheuristic optimizing algorithm is introduced in [15] and analyzing the results reveals its advantages. In order to evaluate the resiliency of MGs in EDNs, unlike previously reviewed articles, three indices are defined in Ref. [16]. Results exhibit that by applying these indices, the resiliency of EDNs is enriched. On the other hand, it is proved that by applying battery energy storage systems along with renewable energy resources, the lost energy is mainly decreased. In Ref. [17], MG formation is considered economically to enhance the resiliency of EDNs. Combination of synchronous DGs with wind turbines, photovoltaic units, and battery energy storage systems are introduced as hybrid MGs and it is proved that hybrid MG formation is a cost-effective method for resiliency improvements.

All the reviewed papers till now focus on resilience enhancement of EDNs by microgrid formation and MG formation is considered as one of the main approaches in achieving resilient EDNs. Other aspects of microgrids formed in EDNs are studied in the following reviewed ones (especially the application of MGs in normal conditions) to show the effectiveness MG formation in both normal and emergency operated EDNs. The bilateral connection of different MGs in a normal operating EDN is studied in [18, 19] based on optimal energy trading among each other. Four MGs are simulated in MATLAB as cooperative MGs in numerical study and the results represent a reduction in load shedding and operational costs. The penetration level of ESSs in MGs is the main goal of Ref. [20] in order to increase the efficiency of microgrids. The objective function of the proposed strategy is to decrease the overall cost of MGs while maintaining their durability and sustainability. The aspects of interconnected MGs are studied in Ref. [21] focusing on voltage stability and loadability. The impact of demand response programs on MGs is also evaluated. The proposed optimizing algorithm is formulated as a mixed-integer nonlinear stochastic problem where the minimization of MGs' operational cost is the main objective function. The results exhibit voltage profile and loadability improvement and loss reduction. Enhancing the resilience of EDNs by MGs seeking for maximum installable PV units is studied in Ref. [22]. In this regard, mobile synchronous DGs are considered and the results reveal that simultaneously taking into account of maximizing PV penetration and dispatch problem of mobile synchronous DGs can lead to a more resiliency. Other aspects of MG formation such as aims, trends, scopes, recommendations, controlling methods, and etc. can be found in [23–26].

1.3. Research gaps and novelties

As it is clear, both active and reactive powers of a system must be controlled whether in normal or emergency conditions and the generated powers must be equal with the consumed ones as the power balance rule. The demand for reactive powers in an EDN is only supplied by synchronous DGs in the emergency operating mode which is not sufficient. According to this fact, some of the loads are curtailed while the extra capacity of active power generation is available. In other words, this insufficiency acts as a constraint and limits the supplying of loads and as a result, the resiliency of EDNs. None of the reviewed articles have paid attention to this issue and no more reactive power-generating device is optimally placed for resiliency improvement of EDNs. A summary of works that are reviewed previously is included in Table 1.

This paper proposes the optimally placement of switchable capacitor banks (SCBs) in the energy management process and evaluates their role in releasing the capacity of renewable resources and resiliency improvement of EDNs. Unlike the non-convex model, the proposed approach is a convex MIQCP one whose solution results in global optimum by the aid of GUROBI solver in GAMS.

1.4. Contribution and paper organization

Reactive power along with active power management can be beneficial in enhancing the resiliency of EDNs especially in emergency operating mode. A formulation methodology included with SCB is proposed as an innovation to improve the resiliency of emergency-operated EDNs. The presented model follows multiple aims, and the main one is the reduction of energy not supplied by releasing more available capacity of optimally installed renewable DGs. The formulations are based on mixed-integer quadratically-constrained programming (MIQCP) and the validating process is done on the IEEE 69-bus system. Shortly, the main outstanding specifications of this paper are as follows:

- Improving the resiliency of EDNs confronted a destructive disaster;

Table 1. Summary of studied works in the reviewed articles.

[Ref.] (Year)	Formulation	Distributed energy resources				Master-slave control	Switchable capacitor banks	Maximum use of renewable resources
		Synchronous DG	WT	PV	ESS			
[4] (2023)	MILP	✓	✓	✓	✓	-	-	-
[5] (2024)	MINLP	✓	-	-	-	-	-	-
[6] (2022)	MILP	-	✓	✓	✓	✓	-	-
[7] (2023)	Heuristic	✓	✓	✓	✓	-	-	-
[8] (2023)	Heuristic	✓	✓	✓	✓	-	-	-
[9] (2021)	MILP	✓	-	✓	✓	-	-	-
[10] (2023)	NLP	✓	-	-	✓	-	-	-
[11] (2023)	MILP	-	-	✓	✓	-	-	-
[12] (2023)	Heuristic	✓	-	✓	✓	-	-	-
[13] (2024)	Heuristic	✓	✓	✓	✓	-	-	-
[14] (2021)	Heuristic	✓	✓	✓	-	-	-	-
[15] (2024)	Heuristic	✓	-	✓	✓	-	-	-
[16] (2023)	Heuristic	-	✓	✓	✓	-	-	-
[17] (2021)	MILP	✓	✓	✓	-	-	-	-
[18] (2024)	Heuristic	✓	✓	✓	✓	-	-	-
[19] (2024)	Heuristic	✓	-	✓	-	-	-	-
[20] (2023)	Heuristic	✓	✓	✓	✓	-	-	-
[21] (2022)	MINLP	✓	✓	✓	✓	-	-	-
[22] (2022)	MILP	✓	-	✓	-	✓	-	-
This study	MIQCP	✓	✓	✓	✓	✓	✓	✓

- Focusing on reactive power management and its corresponding necessities especially;
- Surveying the impacts of reactive power management on releasing renewable resources capacity;
- Considering different strategies for improving the resiliency of EDNs;
- Evaluating the role of SCBs in the resiliency of EDNs.

The rest parts of the paper are organized as follows: Section 2 presents problem formulation which includes numerous sub-sections such as objective function, power flow equations, micro-grid formation, radiality, load shedding, synchronous DG, wind turbine, PV unit, energy storage system, and SCB constraints. In Section 3, the simulation results are evaluated and analyzed. Finally, in Section 4 the main highlighting approaches are concluded.

2. PROBLEM FORMULATION

Essential equations and problem formulations are defined in the following sub-sections. The first part covers the minimizing of load shedding in emergency situations as the objective function. Convex power flow, forming of micro-grid, radiality of system, load curtailment, synchronous DG, wind turbine, photovoltaic, energy storage system, and switchable capacitor bank equations are included in the rest of subdivisions respectively. Also, it should be mentioned that the simulation is implemented in the GAMS environment using the GUROBI solver and all the applied equations are linearized and convex.

2.1. Objective function

The main measuring parameter of EDNs in the case of emergency operation mentioned by literatures is the load shedding. Almost all the studied and proposed methods try to decrease the amounts of load shedding or to supply at least all sensitive loads during this mode. Like previous works, this paper focuses on load shedding as the objective function that must be minimized. On the other hand, maximizing the generation of renewable resources such as wind and PV units is calculated and analyzed and their impact on the load shedding reduction is discussed. The penalty factor of VOLL and priority factor (f) of loads are multiplied by active power load shedding (P^{lsh}), and thus the objective function of this paper is formulated as Eq. (1).

$$OF = \min \left\{ \sum_{t \in \Omega_t} \sum_{i \in \Omega_n} P_{i,t}^{lsh} \times VOLL \times f_i \right\} \quad (1)$$

2.2. Power flow equations

In order to relate the voltage magnitude of buses and the currents passing through the lines, the power flow equations must be modeled. Some researchers proposed a linear form for ordinary AC power flow that can reduce the complexity of the model and lead to a fast runnable one. Thus, the linearized model of power flow proposed in [27] has been applied in the modeling of the problem as Eqs. (2)-(13).

$$\sum_{j \in \Omega_N} A_{ij} P_{i,j,t}^{net} + \sum_{j \in \Omega_N} B_{ij} R_l^{line} C_{i,j,t} + \sigma_i P_i^l = P_{i,t}^G + P_{i,t}^{DG} + P_{i,t}^{WT} + P_{i,t}^{PV} + P_{i,t}^{lsh} + P_{D,i,t} - P_{C,i,t} \quad (2)$$

$$\sum_{j \in \Omega_N} A_{ij} Q_{i,j,t}^{net} + \sum_{j \in \Omega_N} B_{ij} X_l^{line} C_{i,j,t} + \sigma_i Q_i^l = Q_{i,t}^G + Q_{i,t}^{DG} + Q_{i,t}^{CAP} + Q_{i,t}^{lsh} \quad (3)$$

$$-(1 - X_{i,j}) \text{bigM} \leq U_{j,t} + 2(R_l^{line} P_{i,j,t}^{net} + X_l^{line} Q_{i,j,t}^{net}) - U_{i,t} + (R_l^{line^2} + X_l^{line^2}) C_{i,j,t} \leq (1 - X_{i,j}) \text{bigM} \quad (4)$$

$$(P_{i,j,t}^{net^2} + Q_{i,j,t}^{net^2}) \leq C_{i,j,t} U_{j,t} \quad (5)$$

$$P_{i,j,t}^{net} = -P_{j,i,t}^{net} \quad (6)$$

$$Q_{i,j,t}^{net} = -Q_{j,i,t}^{net} \quad (7)$$

$$X_{i,j} = X_{j,i} \quad (8)$$

$$-X_{i,j} P_{min}^{net} \leq P_{i,j,t}^{net} \leq X_{i,j} P_{max}^{net} \quad (9)$$

$$V_{min} \leq V_{i,t} \leq V_{max} \quad (10)$$

$$V_{min} \leq V_{i,t} \leq V_{max} \quad (11)$$

$$(V_{min})^2 \leq U_{i,t} \leq (V_{max})^2 \quad (12)$$

$$0 \leq C_{i,j,t} \leq X_{i,j} (I_{i,j}^{max})^2 \quad (13)$$

Eqs. (2) and (3) cover the active and reactive power balance of the system, respectively. As mentioned before, the master-slave technique is applied to control the frequency of each formed MG. According to this technique, each MG must be included with at least one synchronous DG as the master unit and other units as slave ones in the critical operation of EDNs. The voltage of the two adjacent buses is related by Eq. (4). Eq. (5) relates the main parameters of the system including the nodal powers, voltages, and currents to each other. The amount of sending and receiving active and reactive powers of buses are considered equal by Eqs. (6) and (7). Eq. (8) guarantees a bilateral connection of the existing lines between two buses. The passing active and reactive powers of disconnected lines are fixed to zero by Eqs. (9) and (10). The limitations of the voltage of buses are also presented in Eqs. (11)-(12). The passing current through each line must be lower than its thermal capacity. This issue is expressed by Eq. (13).

2.3. Constraints of micro-grid formation

Microgrid formation as the most effective method that enhances the resiliency of EDNs is applied and modeled by Eqs. (14)-(20). According to the mentioned convex model, the network can be operated in any predefined number of individual islands as microgrids. In this formulation, a binary variable ($a_{i,m}$) is defined to specify the existence of bus i in micro-grid m . Based on this model, each bus of the network must belong to a typical MG at every time (Eq. (14)). In the following, the essential microgrid-forming equations are discussed. In the first step, it should be assumed that each bus and each line of the network belong to only one islanded area (microgrid); this characteristic is defined by Eqs. (15)-(17). To make islanding, any two different islands at time t must not be connected to each other by the lines that exist between them. The linearized model of this issue can be expressed by Eqs. (18)-(20).

$$\sum_{m \in \Omega_{MG}} a_{i,m} \leq 1 \quad (14)$$

$$X_{i,j,m}^{MG} = X_{j,i,m}^{MG} \quad (15)$$

$$\sum_{m \in \Omega_{MG}} X_{i,j,m}^{MG} \leq 1 \quad (16)$$

$$\sum_{m \in \Omega_{MG}} X_{i,j,m}^{MG} = X_{i,j} \quad (17)$$

$$r_{i,j,m}^{pos} + r_{i,j,m}^{neg} \leq (1 - X_{i,j,m}^{MG}) \quad (18)$$

$$a_{i,m} - a_{j,m} = r_{i,j,m}^{pos} - r_{i,j,m}^{neg} \quad (19)$$

$$r_{i,j,m}^{pos} + r_{i,j,m}^{neg} \leq 1 \quad (20)$$

2.4. Radiality constraints

One of the main characteristics of EDN is radial connection of its lines. This characteristic must be confirmed in any operating mode even in emergency conditions. Therefore, to prevent mesh structure and also creation of separated buses in the system, the following two conditions must be checked simultaneously:

- 1) The number of lines must be equal to the number of buses minus one (specified for both normal and critical operations);
- 2) One path must exist from the upstream network to all buses of the distribution system in only normal operation.

The required formulations for satisfying the radiality constraints are specified as Eqs. (21)-(29). Condition (I) is confirmed by Eq. (21). A hypothetical power flow is defined and applied as Eqs. (22)-(26) to satisfy the radial structure of EDNs in any operating mode and condition. When an event occurs and causes the breakdown of an upstream network, the system can be scattered into various individual islands. In this situation, the condition (II) is neglected. Also, Eqs. (27)-(29) ensure the connection of buses to each other in a specified MG.

$$\sum_{l \in \Omega_l} X_{i,j} = 2 \left(\sum_{i \in \Omega_N} i - 1 \right) \quad (21)$$

$$\text{Gen}_{i,m} - 0.1 \times a_{i,m} = \sum_{j \in \Omega_N} \text{flow}_{i,j,m} \quad (22)$$

$$\text{flow}_{i,j,m} + \text{flow}_{j,i,m} = 0 \quad (23)$$

$$\text{flow}_{i,j,m} \leq X_{i,j,m}^{MG} \times \text{bigM} \quad (24)$$

$$\text{flow}_{i,j,m} \geq -X_{i,j,m}^{MG} \times \text{bigM} \quad (25)$$

$$\sum_{i,j \in \Omega_N} X_{i,j,m}^{MG} = 2 \left\{ \sum_{i \in \Omega_N} a_{i,m} - 1 \right\} \quad (26)$$

$$\text{Gen}_{i,m} \leq \gamma_{i,m} \times 100 \quad (27)$$

$$\sum_{i \in \Omega_N} \gamma_{i,m} = 1 \quad (28)$$

$$\sum_{m \in \Omega_{MG}} \sum_{i \in \Omega_N} \gamma_{i,m} = \sum_{m \in \Omega_{MG}} m \quad (29)$$

2.5. Load shedding constraints

In order to balance the generated and consumed powers by the failure of some parts of the network, the concept of load shedding and curtailment is applied. The constraints of load shedding can be defined by Eqs. (30)-(32). The relation of active and reactive loads that can be curtailed is modified by Eq. (30). Eqs. (31) and (32) limit the active and reactive amounts of load curtailments to the maximum load of the determined bus respectively.

$$Q_{i,t}^{lsh} = \left(\frac{Q_i^l}{P_i^l} \right) P_{i,t}^{lsh} \quad (30)$$

$$P_{i,t}^{lsh} \leq \sigma_t P_i^l \quad (31)$$

$$Q_{i,t}^{lsh} \leq \sigma_t Q_i^l \quad (32)$$

2.6. Constraints of SDGs

The limits of active and reactive powers generated by synchronous DGs (SDGs) are expressed in Eqs. (33) and (34). Whereas nonlinearity characteristic of Eq. (33), it cannot be solved by GUROBI solver. Thus, it is substituted by approximated Eqs. (35) and (36), in which, DG_i is a binary variable representing the installation of SDG on bus i , and S_{max}^{DG} indicates the rated capacity of DGs. Also, in Eq. (37) N_{max}^{DG} is the maximum number of available SDGs. The essential master DG constraints in each MG are covered by Eqs. (38)-(44). The voltages of optimally placed master DGs are fixed to 1 per unit (pu) by applying convex Eqs. (45) and (46); and the voltage magnitudes of the remaining buses are maintained within [0.9pu-1.1pu]. Due to the applied model, the square of voltages is considered in the modeling equations. Therefore, the limitations of minimum and maximum bound are taken at 0.81 pu and 1.21 pu respectively.

$$(P_{i,t}^{DG})^2 + (Q_{i,t}^{DG})^2 \leq DG_i \times (S_{max}^{DG})^2 \quad (33)$$

$$-\tan \{\cos^{-1}(\text{PF})\} P_{i,t}^{DG} \leq Q_{i,t}^{DG} \leq \tan \{\cos^{-1}(\text{PF})\} P_{i,t}^{DG} \quad (34)$$

$$P_{i,t}^{DG} \leq DG_i \times S_{max}^{DG} \quad (35)$$

$$Q_{i,t}^{DG} \leq DG_i \times S_{max}^{DG} \quad (36)$$

$$\sum_{i \in \Omega_N} DG_i \leq N_{max}^{DG} \quad (37)$$

$$\sum_{m \in \Omega_{MG}} DG_{i,m}^{MG} \leq N_{max}^{DG} - \sum_{m \in \Omega_{MG}} m + 1 \quad (38)$$

$$\sum_{i \in \Omega_N} DG_{i,m}^{MG} \geq 1 \quad (39)$$

$$\sum_{m \in \Omega_{MG}} DG_{i,m}^{MG} = DG_i \quad (40)$$

$$\sum_{m \in \Omega_{MG}} \sum_{i \in \Omega_N} DG_{i,m}^{island} = \sum_{m \in \Omega_{MG}} m \quad (41)$$

$$\sum_{i \in \Omega_N} DG_{i,m}^{island} = 1 \quad (42)$$

$$DG_{i,m}^{island} \leq DG_{i,m}^{MG} \quad (43)$$

$$a_{i,m} \geq DG_{i,m}^{MG} \quad (44)$$

$$U_{i,t} \leq 1.21 - 0.21 \times DG_i \quad (45)$$

$$U_{i,t} \geq 0.81 + 0.19 \times DG_i \quad (46)$$

2.7. Constraints of wind turbines

The generation constraints of wind turbines are expressed by Eqs. (47)-(49) while the number of wind turbines that can be optimally placed is limited by Eq. (47) according to a predefined allowable number. The generated active power of a wind turbine at every time is also limited by its corresponding maximum extractable power as Eq. (48). On the other hand, the electrical power that is generated by each wind turbine can be calculated by Eq. (49) based on Ref. [28]. According to this equation, if the instantaneous wind speed reaches its lower and upper predefined limits, it gets zero; otherwise, the output power follows a fixed value or a linear relation based on the wind speed.

$$\sum_{i \in \Omega_w} W_i \leq N_{max}^W \quad (47)$$

$$P_{i,t}^W \leq W_i \times P_{i,t}^{W, \text{Capacity}} \quad (48)$$

$$\begin{cases} 0 & ; \forall V_t^{wind} < V_{c-in} \\ P_{rated}^W \left(\frac{V_t^{wind} - V_{c-in}}{V_{rated} - V_{c-in}} \right) & ; \forall V_{c-in} < V_t^{wind} < V_{rated} \\ P_{rated}^W & ; \forall V_{rated} < V_t^{wind} < V_{c-out} \\ 0 & ; \forall V_t^{wind} > V_{c-out} \end{cases} \quad (49)$$

2.8. Constraints of PV units

The producible power of PV cells can be calculated by Eqs. (50)-(54) [28] and the number of PV units that can be optimally placed is limited by (55) according to a predefined allowable number. The generated active power of a PV unit at every time is also restricted by (56) in which $P_{i,t}^{PV, \text{Capacity}}$ indicates the functional capacity of PV at bus i and time t according to the solar radiation values.

$$P_{i,t}^{PV, \text{Capacity}} = N_{PV} \times V_t^g \times I_t^g \times FF \quad (50)$$

$$I_t^g = \text{si}_t \left(I_{sc}^{PV} + K_I (T_t^{cg} - 25) \right) \quad (51)$$

$$V_t^g = V_{oc}^{PV} - K_I \times T_t^{cg} \quad (52)$$

$$T_t^{cg} = T_t^A + \text{si}_t \left(\frac{N_{ot} - 20}{0.8} \right) \quad (53)$$

$$FF = \frac{V_{MMP} \times I_{MMP}}{V_{oc}^{PV} \times I_{sc}^{PV}} \quad (54)$$

$$\sum_{i \in \Omega_{PV}} PV_i \leq N_{max}^{PV} \quad (55)$$

$$P_{i,t}^{PV} \leq PV_i \times P_{i,t}^{PV, \text{Capacity}} \quad (56)$$

2.9. Constraints of ESSs

The related constraints of energy storage systems (ESSs) are defined by Eqs. (57)-(62). Eq. (57) demonstrates the state of charge (SOC) of ESSs at each hour and bus and relates it to the charging and discharging powers. According to Eq. (58), at each time, the storage units must be either charged or discharged. Eqs. (59) and (60) limit the charged or discharged active power of each unit in the available buses. The SOC of each unit is limited to a predefined amount expressed by (61) as SOC_{max} . Also, Eq. (62) equals the SOC of units in the last hour of a day to that of its initial value [27].

$$SOC_{i,t} = SOC_{i,(t-1)} + (P_{C_{i,t}} \times \eta_{ch}) - \left(\frac{P_{D_{i,t}}}{\eta_{dch}} \right) \quad (57)$$

$$ch_{i,t} + dch_{i,t} \leq 1 \quad (58)$$

$$0 \leq P_{C_{i,t}} \leq ch_{i,t} \times P_{max}^{ESS} \quad (59)$$

$$0 \leq P_{D_{i,t}} \leq dch_{i,t} \times P_{max}^{ESS} \quad (60)$$

$$0 \leq SOC_{i,t} \leq SOC_{max} \quad (61)$$

$$SOC_{i,t_{24}} = SOC_{i,t_0} \quad (62)$$

2.10. Constraints of SCBs

Switchable capacitor bank supplies the reactive power of EDNs, and its different aspects have been studied in literature. But, as mentioned before, the role of these electrical devices in improving the resiliency of EDNs has not been studied previously. This paper tries to study its operational behavior in emergency conditions as an innovation. The following equations are used to model the SCBs linearly. Eq. (63) limits the number of SCBs to a predefined number that can be placed optimally. Eq. (64) relates the amount of producible reactive power of capacitor banks to the maximum amounts, and Eq. (65) limits the capacitor banks to the placed SCBs. It is worth mentioning that N_s is the number of switchable steps of SCBs which in this study it is assumed as 3. However, this can be extended to any other different numbers of steps.

$$\sum_{i \in \Omega_{CAP}} Cap_i \leq N_{max}^{Cap} \quad (63)$$

$$Q_{i,t}^{CAP} = \left\{ \frac{(K1_{i,t} + K2_{i,t} + K3_{i,t})}{N_s} \right\} \times S_{max}^{CAP} \quad (64)$$

$$Cap_i \geq \left\{ \frac{(K1_{i,t} + K2_{i,t} + K3_{i,t})}{N_s} \right\} \quad (65)$$

2.11. Solution process of the proposed model

The proposed model has been programmed and executed in GAMS as powerful software for solving optimization problems. The optimization process of the problem can be depicted as Fig. 2.

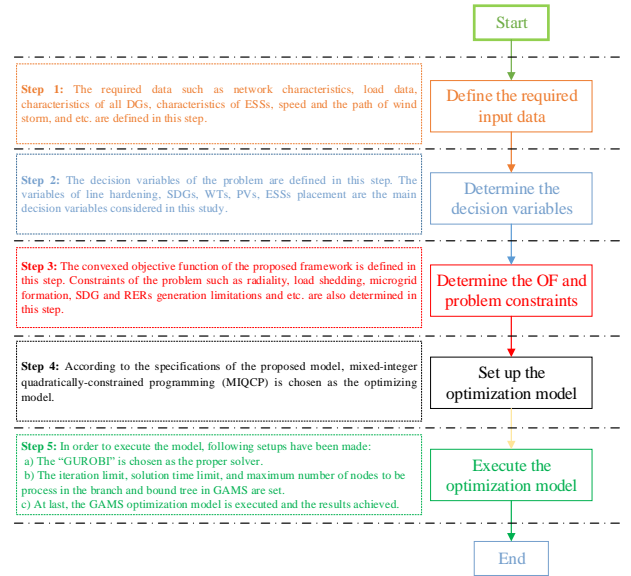


Fig. 2. Conceptual diagram of the proposed framework.

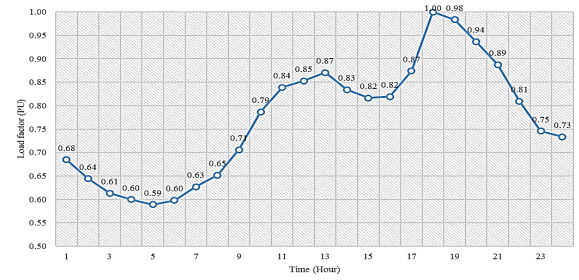


Fig. 3. The system's load profile in a day.

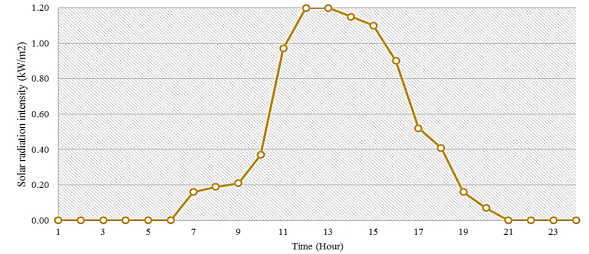


Fig. 4. Intensity of solar radiation in a day.

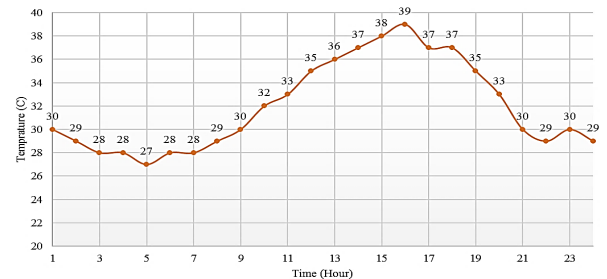


Fig. 5. Ambient temperature in a day.

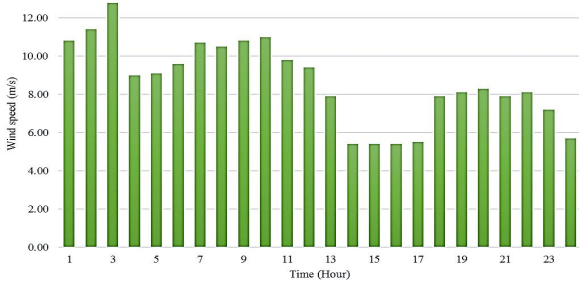


Fig. 6. Wind speed profile in a day.

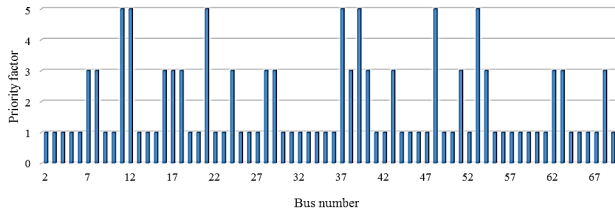


Fig. 7. Considered priority factor of the load of buses.

3. NUMERICAL STUDY

3.1. Input parameters and applied system

In order to evaluate the functionality of the proposed model, the input parameters and the test system are presented in this sub-section. The load profile during the day is exhibited in Fig. 3. Moreover, Figs. 4, 5, and 6 depict the solar radiation, ambient temperature, and wind speed, during the day based on Ref. [29]. Also, the assumed load priority factors for the buses have been shown in Fig. 7. The necessary constant parameters of the system’s devices have been given in Table 2. The charge and discharge efficiencies of ESSs are also assumed 0.95 and 0.9, respectively.

The validation of the proposed model is fulfilled on the IEEE 69-bus system. More information about this system can be found in [30]. The proposed framework was modeled in the GAMS environment using the GUROBI solver considering. It should be mentioned that MIQCP formulations can be solved by various global optimum solvers (such as CPLEX, GUROBI and etc.). Among the mentioned ones, GUROBI is chosen and applied due to its higher solving speed. The simulations are executed on a

Table 2. Specifications of system’s components considered in the study.

System	Parameter	Value/(Unit)
WT	P_{rated}	100 kW
	V_{c-in}	4 m/s
	V_{c-out}	25 m/s
	V_{rated}	14 m/s
	V_{MMP}	28.66 V
PV	I_{MMP}	7.76 A
	V_{oc}^{PV}	36.96 V
	I_{sc}^{PV}	8.38 A
	N_{ot}	43 °C
	K_I	0.00545 A/°C
	K_v	0.1278 V/°C
	N_{PV}	491
ESS	SOC_{max}	0.5 MWh
	P_{ESS}^{max}	0.1 MW
	$SOC_{i^{min}, s^{min}, t_0}$	0.3 SOC_{max}
SCB	S_{max}^{SCAP}	100 kVAr
	Steps	3
DG	S_{max}^{SDG}	400 kW
	PF	0.8
Network	I_{i^j, v^j}^{max}	250 A

personal computer with Intel Core i5 CPU @ 4 GHz, and 8 GB RAM. It should be noted that the meta-heuristic-based algorithms such as genetic algorithm (GA), particle swarm optimization (PSO), etc., can be also used for solving the optimization problems. But as these algorithms are based on iterative process without mathematical methods, the solutions obtained by them are usually local optima not the global optimum. In the meta-heuristic algorithms, the quality of solutions is dependent on the algorithm’s parameters. For example in the GA, the parameters include the number of population, cross-over rate, mutation rate, etc. But, the proposed model of this paper is obtained using mathematic-based solvers in the GAMS where there is no any special parameter for tuning. Specifically for the convex models, no matter how many times the optimization is performed, the solution will be the same if the global optimum solvers such as “GUROBI” are used [31].

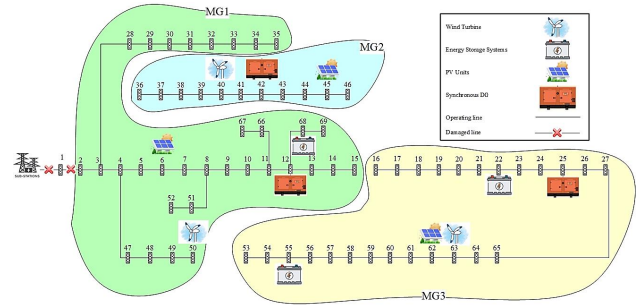


Fig. 8. Schematic view of the system damaged by a disaster-Case 1.

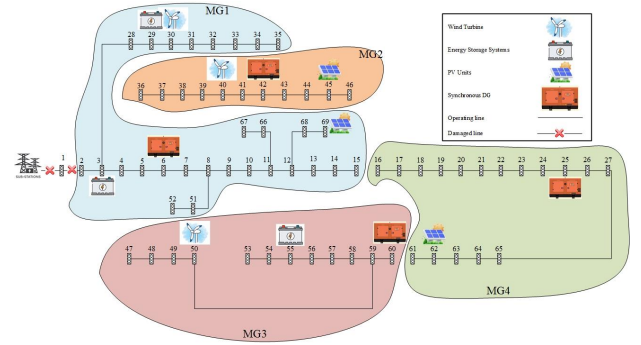


Fig. 9. Schematic view of the system damaged by a disaster-Case 2.

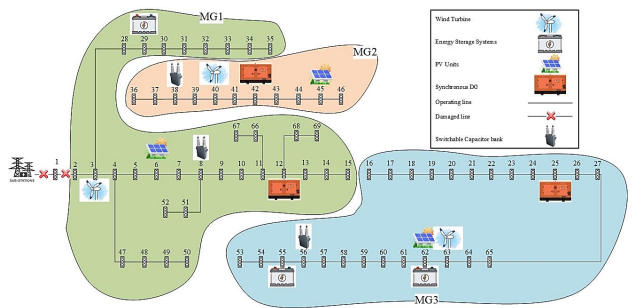


Fig. 10. Schematic view of the system damaged by a disaster-Case 3.

3.2. Simulation results and discussion

The following three case studies are implemented on the test system to analyze the performance of the proposed model.

Table 3. Simulation results obtained for each case.

No. of Cases	SDG	WT	PV	SCB	Cost (\$)	WT (MWh)	PV (MWh)	Loss (MW)	OF (MWh)
Case 1	3	3	3	0	1969200	1.135	0.457	0.138	80.806
Case 2	4	3	3	0	2375600	1.171	0.978	0.152	68.262
Case 3	3	3	3	3	2001000	3.351	2.223	0.102	69.821

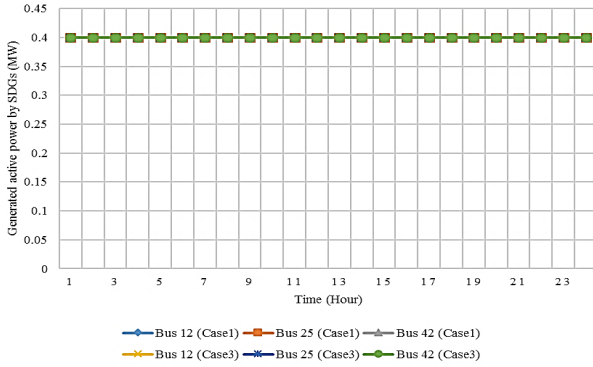


Fig. 11. Generated active power by optimally placed SDGs-Cases 1 & 3.

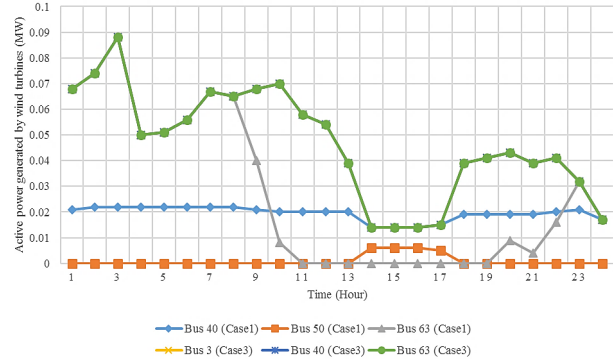


Fig. 14. Generated active power by optimally placed wind turbines-Cases 1 & 3.

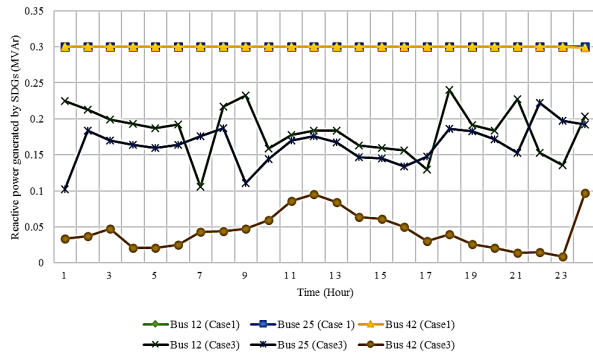


Fig. 12. Generated reactive power by optimally placed SDGs-Cases 1 & 3.

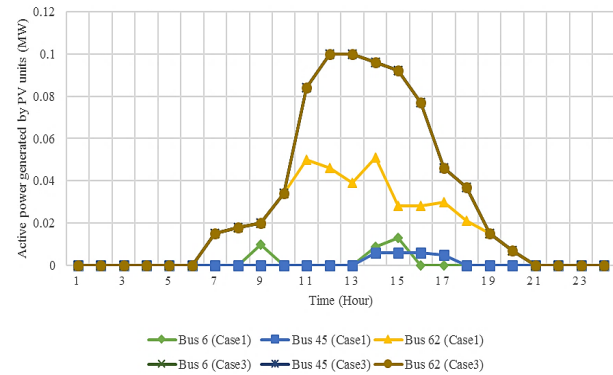


Fig. 15. Generated active power by optimally placed PV units-Cases 1 & 3.

Case 1: The disaster has affected the test system and the network includes 3 SDG devices, 3 wind turbines, and 3 PV units. SCBs are not included in this case.

Case 2: The disaster has affected the test system and the network includes 4 SDG devices, 3 wind turbines, and 3 PV units. SCBs are not included in this case.

Case 3: The disaster has affected the test system and the network includes 3 SDG devices, 3 wind turbines, 3 PV units, and 3 SCBs.

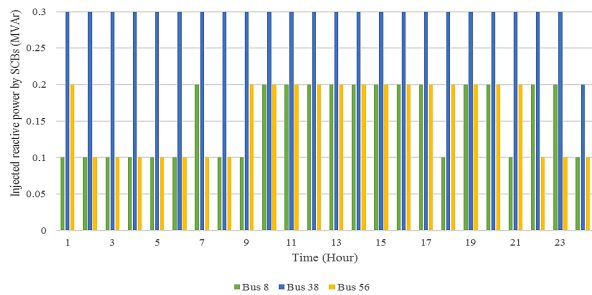


Fig. 13. Injected reactive power by optimally placed SCBs.

The simulation results of different case studies are summarized in Table 3. Also, the investment costs of different system devices are calculated per each case and included in Table 3 based on

[32, 33]. Comparing the results of the mentioned case studies reveals that cases 2 and 3 nearly have the lowest amount of load shedding but case 2 against case 3 is not economic and the penetration level of RERs is not acceptable and meaningful in emergency-operated EDN. More electrical loss and more air-polluting generation of SDGs are other deficiencies belonged to this case. On the other hand, the difference in load shedding in cases 2 and 3 is very small and it can be neglected. However, the investment cost of installed devices in case 3 is lower than in case 2 about 15.77% and the generated energies of wind turbines and PV units are more than in case 2 by about 286.16% and 227.3% respectively. Also, case 3 in comparison with case 1 has several advantages including lower objective function about 13.6% and lower loss about 26.1% and higher penetration level of renewable resources about 285.6%. The difference in investment costs is very small and can be neglected too. Therefore, according to the named advantages of case 3 over other methods, this case (case 3) which can be called as the innovation of this paper, is proposed and analyzed precisely in the following. Due to the multiplicity of the figures and also to better evaluate the performance of case 3, the results are compared with case 1 correspondingly.

The schematic views of the test system in the mentioned cases are shown in Figs. 8, 9, and 10 respectively. The supplied loads of each MG along with optimally placed SDGs, WTs, PV units,

Table 4. The total load shedding of the system at 6:00 PM.

Case	Plsh (MW)	Qlsh (MVar)
1	2.90	2.05
3	2.66	1.89

ESSs, and SCBs are also included in these figures. Undertaking the results reveals that the numbers of formed MGs are different among the considered cases. In which, the number of MGs in cases 1 and 3 is 3 and the number of MGs in case 2 is 4 due to the predefined numbers of SDGs. This difference leads to different expanse of supplying loads by each MG. As an example, it can be seen that MGs in case 2 supply more loads compared with cases 1 and 3. Also, each formed MG includes at least one SDG as a master unit and other types of DGs and ESSs as slave ones.

The figure of generated active powers by SDGs is depicted in Fig. 11. As it is clear, all the SDGs work at their maximum capacity in both cases to minimize the objective function. Also, generated reactive powers by SDGs are shown in Fig. 12, in which the amounts of generated reactive powers by SDGs as the only reactive power sources are at the highest level in case 1. On the other hand, these amounts are decreased in case 3 by optimal placement of SCBs.

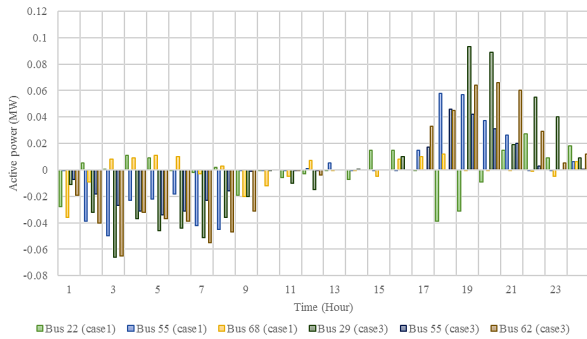


Fig. 16. Charge/discharge active power by ESSs-Cases 1 & 3.

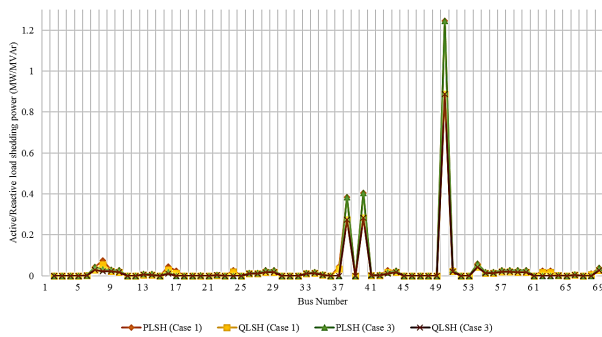


Fig. 17. Active and reactive load shedding power at 6:00 PM-Cases 1 & 3.

The optimally switched SCB steps per hour of operating period is shown in Fig. 13. Almost all the steps of SCB in bus 38 are switched and this issue caused a decrease of generated reactive power by SDG placed in bus 42 and MG2. Approximately, the two other SCBs work similarly. Figs. 14 and 15 show the generated active powers by WTs and PV units respectively. Both WTs and PV units are in their maximum generating available capacity in case 3 while these capacities cannot be reached to their highest level according to reactive power limitations. In other words, by managing the reactive power of the system even in contingency conditions, more penetration levels of renewable resources are available.

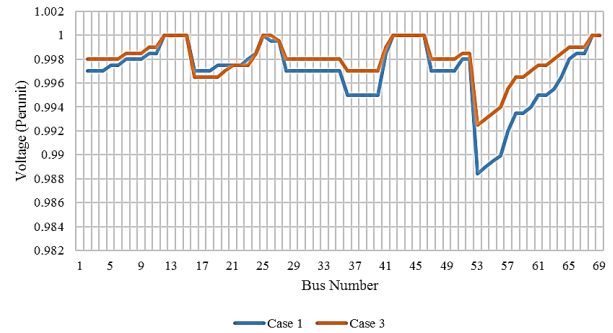


Fig. 18. Voltage profile of the network at 6:00 PM-Case 3.

The depicted Figs. 14 and 15 testify the mentioned increase penetration level of RERs. All the available capacities of wind turbines placed in buses 3, 40 and 63 are dispatched in case 3 while the small amounts of these units optimally placed in buses 40, 50 and 63 are injected to the network in case 1. This issue is true for PV units too. The whole available capacities of PV units placed in buses 6, 45 and 62 are injected to the network in case 3 while the corresponding amounts in case 1 are close to zero even during 11:00 AM to 5:00 PM.

Another superiority of case 3 over case 1 is the higher usage of ESSs in energy management of an emergency-operated EDN. This issue is shown in Fig. 16. As it is clear, the higher amounts of charging and discharging modes belong to case 3. The negative amounts present the charging mode and positive amounts present the discharging mode. ESSs are mostly charged from 2:00 AM to 9:00 AM in which the load of the system is lower and the wind generation is more available. By increasing the amounts of system’s load, they are mostly discharged from 5:00 PM to 10:00 PM. Also, it should be mentioned that the active power of PV units is directly injected to the network because of small amounts of stored energy during 10:00 AM to about 5:00 PM in both cases.

The values of active and reactive load shedding are shown in Fig. 17. The model in both case studies tries to supply the sensitive loads such as loads in buses 11 and 12. However, the system in case 3 decreases the amounts of curtailed loads with middle priority factor (priority 3) in comparison with case 1. As an example, the load shedding amounts of loads in buses 8 and 62 possessed priority 3 is lower in case 3 compared to their corresponding amounts in case 1 and etc. The total amounts of active and reactive load shedding are included in Table 4. Comparing the results of cases 1 and 3 reveals that by applying the proposed method (case 3) the total amounts of active and reactive powers of loads at 6:00 PM are decreased about 8.28% and 7.8% respectively.

The profile of voltage is depicted in Fig. 18 according to the two different cases. As it can be seen, both cases observe the predefined limitations of voltage but the voltage profile of case 3 is smoother than that of case 1. In other words, increasing the penetration levels of RERs and reactive management of SCBs, the quality of the delivered energy is also improved.

4. CONCLUSION

Due to changing climate conditions globally and the increasing frequency of high-impact, low-probability disasters, improving the resiliency of EDNs is vital. In this paper, a novel economic enhancement framework was proposed, considering reactive power management through switchable capacitors. The essential modeling formulations were linearized, and the model was solved as an MIQCP, minimizing load shedding as the objective function. The specifications of this model were studied and analyzed using the IEEE 69-bus test system. Results confirmed that the proposed framework can improve the durability of EDNs and enhance their

resiliency economically by deploying switchable capacitor banks. In summary, it can be concluded:

- The proposed framework improves the resiliency of EDNs. To achieve this, the amount of load shedding was compared across scenarios, showing a 13.6% decrease in load shedding for the case equipped with SCBs.
- The proposed convex model enhances the role of ESSs in improving resiliency.
- Mitigating reactive power limitations using switchable capacitor banks in an EDN can unlock the potential of renewable resources, even in emergency conditions. A comparison of the results revealed that with SCBs, the penetration level of renewable energy resources (RERs) increased by approximately 285.6%.
- The quality of delivered energy improves in scenarios involving SCBs.

For future research, the proposed scheme will incorporate uncertainty modeling of natural disasters, as well as mobile synchronous DGs and energy storage systems. It will also consider integrating electric vehicles as generating resources in emergency modes, and explore other reactive compensating devices, such as SVC and power electronics-based solutions, which are not addressed in this study but will be investigated in future research. Additionally, the consideration of problem uncertainties (including load, renewable energy generation, and disaster behavior) could be another promising avenue for future studies.

REFERENCES

- [1] H. A. Abdelsalam, A. Eldosouky, and A. K. Srivastava, "Enhancing distribution system resiliency with microgrids formation using weighted average consensus," *Int. J. Electr. Power Energy Syst.*, vol. 141, p. 108161, 2022.
- [2] M. Borghei and M. Ghassemi, "Optimal planning of microgrids for resilient distribution networks," *Int. J. Electr. Power Energy Syst.*, vol. 128, p. 106682, 2021.
- [3] F. Amini, S. Ghassemzadeh, N. Rostami, and V. S. Tabar, "A stochastic two-stage microgrid formation strategy for enhancing distribution network resilience against earthquake event incorporating distributed energy resources, parking lots and responsive loads," *Sustainable Cities Soc.*, vol. 101, p. 105191, 2024.
- [4] I. M. Diahovchenko, G. Kandaperumal, and A. K. Srivastava, "Enabling resiliency using microgrids with dynamic boundaries," *Electr. Power Syst. Res.*, vol. 221, p. 109460, 2023.
- [5] R. Sheikhejad, G. Gharehpetian, and H. Rastegar, "Active distribution network expansion planning considering microgrids for supplying critical loads," *Sustainable Energy Grids Networks*, vol. 38, p. 101281, 2024.
- [6] M. A. Gilani, R. Dashti, M. Ghasemi, M. H. Amirioun, and M. Shafie-khah, "A microgrid formation-based restoration model for resilient distribution systems using distributed energy resources and demand response programs," *Sustainable Cities Soc.*, vol. 83, p. 103975, 2022.
- [7] W. Mingming, L. Zhaoheng, and M. Konstantin, "Optimal risk-driven operation of renewable-penetrated distribution network during natural-disasters: A resiliency-oriented analysis," *Sustainable Cities Soc.*, vol. 99, p. 104967, 2023.
- [8] X. Chen, J. Zhai, Y. Jiang, C. Ni, S. Wang, and P. Nimmeggers, "Decentralized coordination between active distribution network and multi-microgrids through a fast decentralized adjustable robust operation framework," *Sustainable Energy Grids Networks*, vol. 34, p. 101068, 2023.
- [9] R. Wu and G. Sansavini, "Active distribution networks or microgrids? optimal design of resilient and flexible distribution grids with energy service provision," *Sustainable Energy Grids Networks*, vol. 26, p. 100461, 2021.
- [10] M. I. Anam, T.-T. Nguyen, and T. Vu, "Risk-based preventive energy management for resilient microgrids," *Int. J. Electr. Power Energy Syst.*, vol. 154, p. 109391, 2023.
- [11] A. D. Bintoudi and C. Demoulias, "Optimal isolated microgrid topology design for resilient applications," *Appl. Energy*, vol. 338, p. 120909, 2023.
- [12] J. Lee, G. Razeghi, and S. Samuelsen, "Utilization of battery electric buses for the resiliency of islanded microgrids," *Appl. Energy*, vol. 347, p. 121295, 2023.
- [13] W. Cao and L. Zhou, "Resilient microgrid modeling in digital twin considering demand response and landscape design of renewable energy," *Sustainable Energy Technol. Assess.*, vol. 64, p. 103628, 2024.
- [14] P. Agrawal, N. Kanwar, N. Gupta, K. Niazi, and A. Swarnkar, "Resiliency in active distribution systems via network reconfiguration," *Sustainable Energy Grids Networks*, vol. 26, p. 100434, 2021.
- [15] A. Azizvahed, K. Gholami, G. V. Rupf, A. Arefi, C. Lund, J. Walia, M. M. Rahman, M. R. Islam, S. Muyeen, and I. Kamwa, "Cooperative operational planning of multi-microgrid distribution systems with a case study," *Energy Rep.*, vol. 11, pp. 2360–2373, 2024.
- [16] M. Gholami, S. Muyeen, and S. A. Mousavi, "Development of new reliability metrics for microgrids: Integrating renewable energy sources and battery energy storage system," *Energy Rep.*, vol. 10, pp. 2251–2259, 2023.
- [17] J. Marqusee, W. Becker, and S. Ericson, "Resilience and economics of microgrids with pv, battery storage, and networked diesel generators," *Adv. Appl. Energy*, vol. 3, p. 100049, 2021.
- [18] Z. Ullah, H. S. Qazi, A. Alferidi, M. Alsolami, B. Lami, and H. M. Hasanien, "Optimal energy trading in cooperative microgrids considering hybrid renewable energy systems," *Alexandria Eng. J.*, vol. 86, pp. 23–33, 2024.
- [19] M. Tariq, S. A. A. Kazmi, A. Altamimi, Z. A. Khan, B. Alharbi, H. Alafnan, and H. Alshehry, "Smart transactive energy based approach for planning and scheduling in multi-looped microgrid distribution network across planning horizon," *Heliyon*, vol. 10, no. 5, 2024.
- [20] Q. Hu, G. Zhao, J. Hu, and N. Razmjooy, "Maximizing energy storage in microgrids with an amended multi-verse optimizer," *Heliyon*, vol. 9, no. 11, 2023.
- [21] D. K. Raju, R. S. Kumar, L. P. Raghav, and A. R. Singh, "Enhancement of loadability and voltage stability in grid-connected microgrid network," *J. Cleaner Prod.*, vol. 374, p. 133881, 2022.
- [22] J. M. Home-Ortiz, O. D. Melgar-Dominguez, J. R. S. Mantovani, and J. P. Catalao, "Pv hosting capacity assessment in distribution systems considering resilience enhancement," *Sustainable Energy Grids Networks*, vol. 32, p. 100829, 2022.
- [23] M. Yadav, N. Pal, and D. K. Saini, "Low voltage ride through capability for resilient electrical distribution system integrated with renewable energy resources," *Energy Rep.*, vol. 9, pp. 833–858, 2023.
- [24] N. F. P. Dinata, M. A. M. Ramli, M. I. Jambak, M. A. B. Sidik, and M. M. Alqahtani, "Designing an optimal microgrid control system using deep reinforcement learning: A systematic review," *Eng. Sci. Technol. Int. J.*, vol. 51, p. 101651, 2024.
- [25] A. Akter, E. I. Zafir, N. H. Dana, R. Joysoyal, S. K. Sarker, L. Li, S. Muyeen, S. K. Das, and I. Kamwa, "A review on microgrid optimization with meta-heuristic techniques: Scopes, trends and recommendation," *Energy Strategy Rev.*, vol. 51, p. 101298, 2024.
- [26] F. Alasali, S. M. Saad, A. S. Saidi, A. Itradat, W. Holderbaum, N. El-Naily, and F. F. Elkuwafi, "Powering up microgrids: A comprehensive review of innovative and intelligent protection approaches for enhanced reliability," *Energy Rep.*, vol. 10, pp. 1899–1924, 2023.

- [27] S. Behzadi and A. Bagheri, "A convex micro-grid-based optimization model for planning of resilient and sustainable distribution systems considering feeders routing and siting/sizing of substations and dg units," *Sustainable Cities Soc.*, vol. 97, p. 104787, 2023.
- [28] N. M. Tabatabaei, S. N. Ravadanegh, and N. Bizon, "Power systems resilience," *Switz.: Springer*, 2018.
- [29] S. Behzadi, A. Bagheri, and A. Rabiee, "Resilience-oriented operation of micro-grids in both grid-connected and isolated conditions within sustainable active distribution networks," *ArXiv Prepr. ArXiv:2403.19147*, 2024.
- [30] S. Sivakumar, S. B. Ramasamy Gunaseelan, M. V. Reddy Krishnakumar, N. Krishnan, A. Sharma, and A. Aguila Téllez, "Analysis of distribution systems in the presence of electric vehicles and optimal allocation of distributed generations considering power loss and voltage stability index," *IET Gener. Trans. Distrib.*, vol. 18, no. 6, pp. 1114–1132, 2024.
- [31] A. Soroudi, *Power system optimization modeling in GAMS*, vol. 78. Springer, 2017.
- [32] S. Zhang, H. Cheng, D. Wang, L. Zhang, F. Li, and L. Yao, "Distributed generation planning in active distribution network considering demand side management and network reconfiguration," *Appl. Energy*, vol. 228, pp. 1921–1936, 2018.
- [33] A. Eid, "Cost-based analysis and optimization of distributed generations and shunt capacitors incorporated into distribution systems with nonlinear demand modeling," *Expert Syst. Appl.*, vol. 198, p. 116844, 2022.